DOI: https://doi.org/10.15276/aait.04.2020.4
UDC 004.9 + 616-079.4

CLASSIFICATION OF BRAIN MRI IMAGES BY USING THE AUTOMATIC SEGMENTATION AND TEXTURE ANALYSIS

Anastasia V. Karliuk[1)]
ORCID: https://orcid.org/0000-0001-7011-7237, karliukanastasia@gmail.com
Ievgen A. Nastenko[1)]
ORCID: https://orcid.org/0000-0002-1076-9337, nastenko.e@gmail.com
Olena K. Nosovets[1)]
ORCID: https://orcid.org/0000-0003-1288-3528, o.nosovets@gmail.com
Vitalii O. Babenko[1)]
ORCID: https://orcid.org/0000-0002-8433-3878, vbabenko2191@gmail.com
[1)] National Technical University of Ukraine "Igor Sikorsky Kyiv Polytechnic Institute", 5a Mikhail Braichevsky St. Kyiv, Ukraine

ABSTRACT

Brain tumor is a relatively severe human disease type. Its timely diagnosis and tumor type definition are an actual task in modern medicine. Lately, the segmentation methods on 3D brain images (like computer and magnetic resonance tomography) are used for definition of a certain tumor type. Nevertheless, the segmentation is usually conducted manually, which requires a lot of time and depends on the experience of a doctor. This paper looks at the possibility of creating a method for the automatic segmentation of images. As a training sample, the medical database of MRI brain tomography with three tumor types (meningioma, glioma, and pituitary tumor) was taken. Taking into account the different slices, the base had: 708 examples of meningioma, 1426 examples of glioma, and 930 examples of pituitary tumor. The database authors marked the regions of interest on each image, which were used as a tutor (supervised learning) for automatic segmentation model. Before model creation, currently existing popular automatic segmentation models were analyzed. U-Net deep convolution neural network architecture was used as the most suitable one. As the result of its use, the model was obtained, which can segment the image correctly in seventy four percent of six hundred images (testing sample). After obtaining the automatic segmentation model, the Random Forest models for three "One versus All" tasks and one multiclass task were created for brain tumor classification. The total sample was divided into training (70 %), testing (20 %), and examining (10 %) ones before creating the models. The accuracy of the models in the examining sample varies from 84 to 94 percent. For model classification creation, the texture features were used, obtained by texture analysis method, and created by the co-authors of the Department of Biomedical Cybernetics in the task of liver ultrasound image classification. They were compared with well-known Haralick texture features. The comparison showed that the best way to achieve an accurate classification model is to combine all the features into one stack.

Keywords: Classification; "One Versus All"; Multiclass Task; Automatic Segmentation; Texture Analysis; Tumor; Magnetic Resonance Imaging

For citation: **Anastasia V. Karliuk, Ievgen A. Nastenko, Olena K. Nosovets, Vitalii O. Babenko. Classification of Brain MRI Images by Using the Automatic Segmentation and Texture Analysis. *Applied Aspects of Information Technology.* 2020; Vol.3 No.4: 263–275. DOI:https://doi.org/10.15276/aait.04.2020.4**

INTRODUCTION. FORMULATION OF THE PROBLEM

Nowadays, 3D images, which are taken with the help of structural visualization methods i.e. computer tomography (CT) and magnetic resonance imaging (MRI), are widely used for anatomical abnormalities in clinical practice [1]. These images, if processed correctly and clear processed, give detailed and structured information about pathology or tumor anatomy and can be used for diagnostics and therapy.

There are different methods for tumor size measurement [2]. Manual method depends on human experience and contextual knowledge and can be time consuming and subjective. In comparison, (semi) automatic methods are designed for more reliable and quick volume segmentation.

Modern methods from different image segmentation paradigms (by threshold value,graph-based, region-based, statistic modeling, contour-based, gradient-based, etc.) are adapted and tested for complicated task solving of volume determination. The absence of comparative analysis data leads to the situation, when each method was evaluated on different data and compared only to a limited number of others, hence there was no consensus about the most perspective 3D image segmentation methods [3]. Respectively, there are systems only for image segmentation with mathematical method with further image manual processing at the moment.

Thus, the task of determining the most effective method of automatic segmentation is becoming relevant, which will be used to create automatic systems for recognizing and identifying tumor types from MRI or CT images. It is also very important to

get valuable information from segmented images, which will allow determining the tumor type with high precision.

ANALYSIS OF THE LATEST RESEARCH AND PUBLICATIONS

Despite the wide use of MRI, structural visualization is not ideal for pathology identification, where the cell activity is more important than anatomical features [4]. The necessity of functional characteristics leads to the development of positron emission tomography scanners (PET), which can provide molecular information about the biology of many diseases. In a combination with MRI, the use of functional and structural information gives the possibility to classify the disease more precisely. This way, MRI-PET imaging (not just MRI) is used in modern medicine.

In order to select necessary volume objects, the so-called segmentation is used, which solves the task of recognition [5] (definition process about object location and its difference from other objects on the image) and differentiation [6] (definition of object area dimensional length on the image). It should be taken into account that since doctors perform manual segmentation in 2D images [7] (which are slices of the original 3D images) when solving the task of automatic segmentation of volumetric objects it is reduced to segmentation of several slices in 2D [8], after which the results on all slices of a particular patient determine the volume.

The task of automatic segmentation of medical images is currently one of the most common in Deep Learning. There are different approaches to solving such tasks. One of them is determining the threshold for segmentation. This approach was successfully applied in work [9]. It is simple and intuitive and makes it possible to turn grey tone images into binary images, defining all pixels larger than a certain value as the foreground and all others as the background. The probability of grayscale gradation is usually used to determine thresholds by constructing a histogram of the image. There is also a stochastic approach, which uses the differences between absorption areas and the background.

Among the different methods of this approach, it can be distinguished:

- Fuzzy Locally Adaptive Bayseian (FLAB) segmentation, based on Bayesian statistics [10].
- Classification methods, which divide the space of features receiving from an image using data with known labels [11] (usually using *k*-nearest neighbors (KNN) [12], support vector machine (SVM) [13], etc.
- Clustering methods that aim to collect subjects with similar properties, using spatial information but without training data [14] (quite well-known methods are Fuzzy c-means [15] and spectral clustering [16]).

It is also worth mentioning the region-based segmentation methods that were successfully applied in works [17, 18], as well as border-based methods [19, 20], [21]. However, despite the rather clear principle of these methods and their successful application in specific tasks, in general, the best solution for automatic segmentation of medical images is considered to be the use of neural network convolution [22]. At present, the most effective architecture for a deep convolution neural network of automatic segmentation is U-Net [23] (Fig. 1). It is already considered one of the standards in such tasks and is used not only to define the class of a complete image but also to segment its areas class by class, thus creating a mask that will divide images into several classes.

The U-net network was learned with end-to-end method on a small image set and becomes more successful, than the previous best segmentation method (convolution neural network with shiftable window) in the competition on neural network segmentation in submicroscopic stacks (link: *https://biomedicalimaging.org/2015/program/isbi-challenges/*). U-Net architecture network works relatively fast and 512x512 image segmentation takes less than a second when a modern graphic processor is used [24].

The characteristics of the U-net:

1. Achieving high results in various real-world tasks, especially for biomedical ones.

2. Using small amounts of data to achieve good results.

The network architecture (Fig. 1) consists of a narrowing block (left) and an expansion path (right). The narrowing block is a typical architecture of a convolution neural network. It consists of reapplying two 3x3 bundles, followed by ReLU activation and MaxPooling (2x2) to reduce expansion.

As for automatic segmentation systems, there are not so many of them in the world now. More recently, an automatic TongueNet system was created based on the U-Net neural network [25], which was created for automatic tongue segmentation. Also, a system for the segmentation of breast masses in breast digital tomosynthesis images was made based on the same U-Net [26]. Unfortunately, at the moment there are no systems for automatic segmentation in Ukraine, and doctors do the segmentation manually.

ISSN 2663-0176 (Print)
ISSN 2663-7731 (Online)

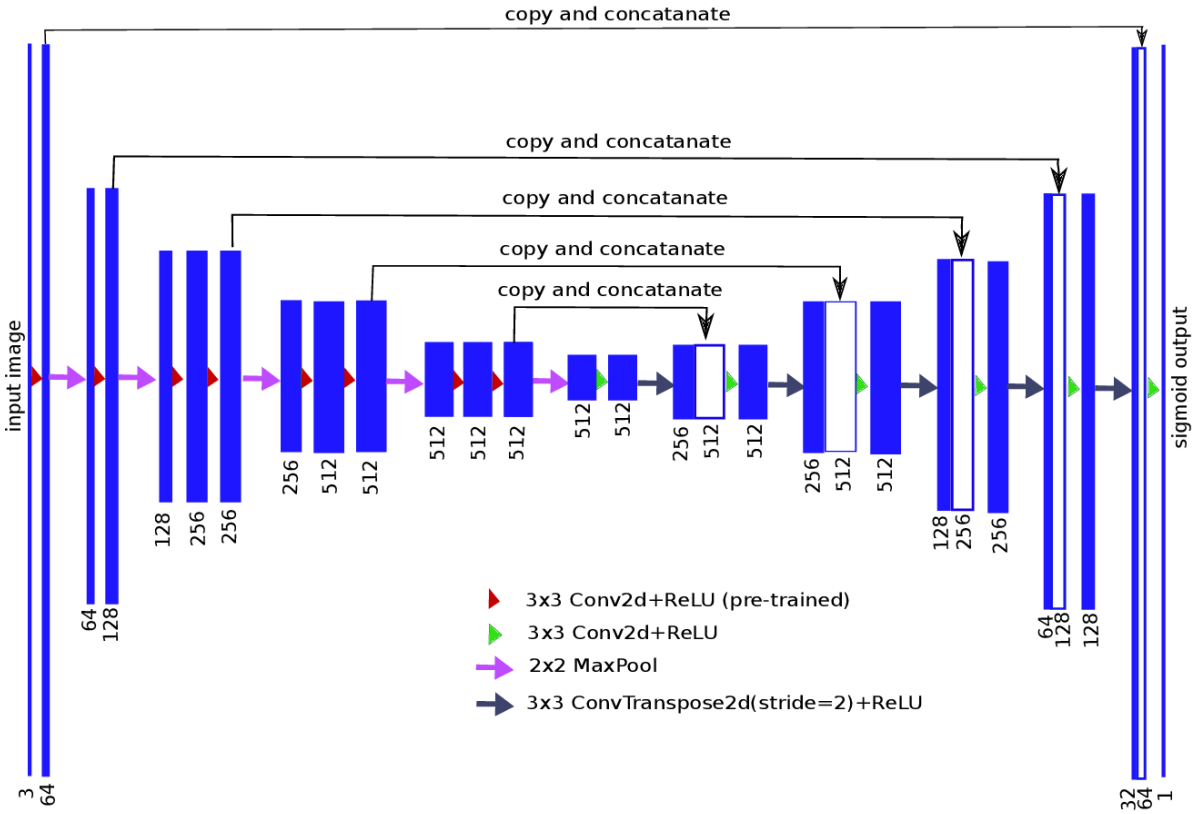

Fig. 1. **U-Net architecture**
***Source*: [23]**

RESEARCH OBJECTIVE

This study aims to create a deep convolution neural network for automatic segmentation of brain MRI images.

The best at the moment U-Net architecture will be used. For this study, 3064 brain MRI images of 512x512 pixels were taken, with a contrast of three types of neoplasms:

1. Meningioma – the tumor that grows from the cells of the spider web of the brain, namely the arachnoid endothelium.

2. Glioma – the tumor that is part of a heterogeneous group and has neuro-ectodermal origins (this tumor is the most common among primary brain tumors).

3. pituitary tumor – the abnormal neoplasm that develops in the pituitary gland.

The data was taken from the following link: *https://figshare.com/articles/brain_tumor_dataset/1512427* [27, 28]. Examples of MRI images with three types of neoplasm are shown in Fig. 2.

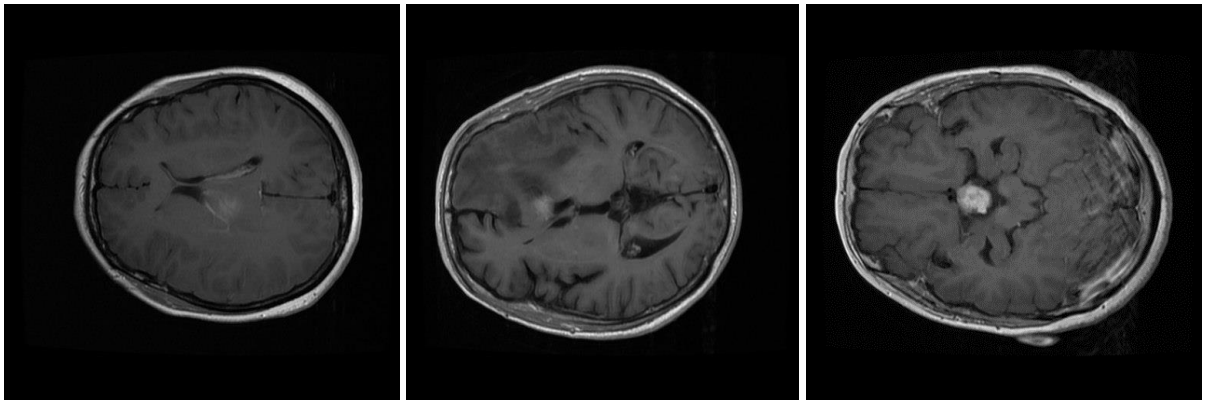

a **b** **c**

Fig. 2. **Example of MRI images of:**
a – meningioma; b – glioma; c – pituitary tumor
***Source*: https://figshare.com/articles/brain_tumor_dataset/1512427**

For each patient, several slices were taken from the original three-dimensional image to create a larger clinical base, resulting in a base that consists of: 708 examples of meningioma, 1426 examples of glioma, and 930 examples of pituitary tumor.

The database authors [27, 28] made manual image segmentation in order to select the region of interest (ROI) for all images. The example of ROI selection is shown in Fig. 3.

ROI is shown as a binary mask, which includes only pixels of white color, while the rest of image area is in black pixels. They were used for automatic segmentation model supervised learning.

Once the automatic segmentation model has been obtained, an equally important task is to build an MRI classification model of images based on the obtained segregated images. To obtain valuable information about images, the classification will be based on texture features proposed by colleagues from the Department of Biomedical Cybernetics at the Igor Sikorsky KPI [29, 30].

TRAINING OF THE MODEL FOR AUTOMATIC SEGMENTATION

Automatic segmentation model was learned on Nvidia GTX 1050Ti 4 GB graphic processor. The total time, spent on the model learning, was 6 hours and 49 minutes. The initial learning rate was 1e-3 and it decreases step by step for 85 % on the plateau, and afterward, the final learning rate was 2.7249e-4 at the end of 100 epochs. In Fig. 4, the learning rate change is shown accordingly to each epoch.

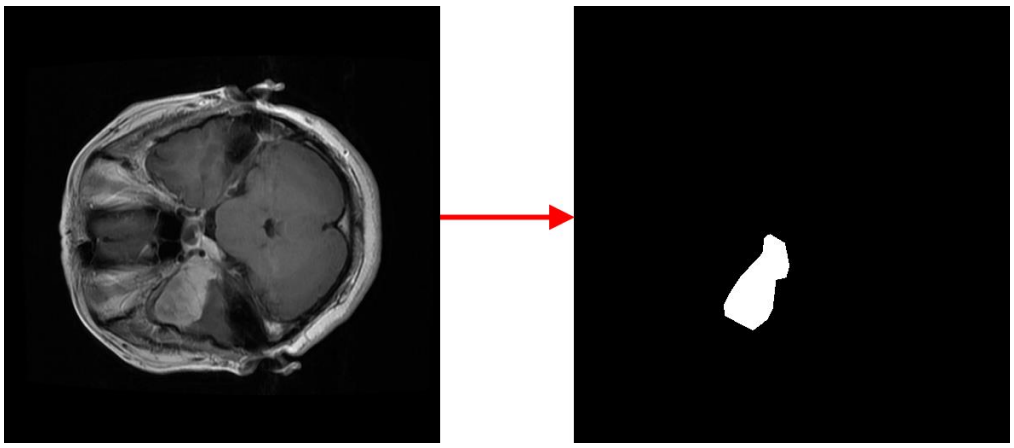

Fig. 3. **Example of manual segmentation of MRI image**
***Source*: https://figshare.com/articles/brain_tumor_dataset/1512427**

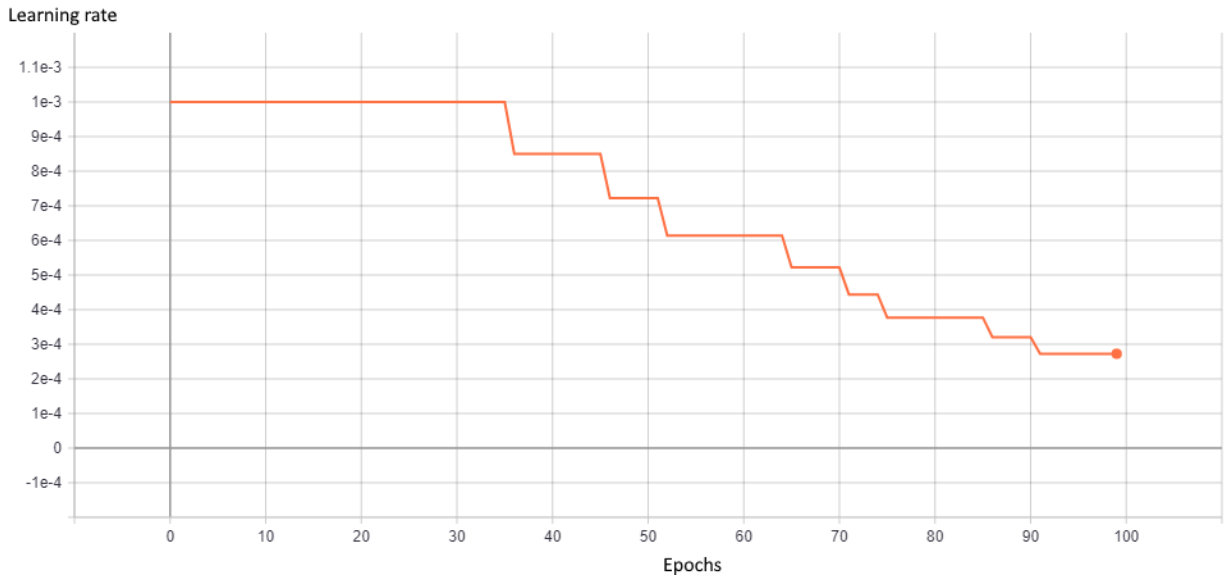

Fig. 4. **Learning rate changing by epochs**
***Source*: compiled by the author**

ISSN 2663-0176 (Print)
ISSN 2663-7731 (Online)

In Fig. 5, error variation (loss function) of predicted segmentation in comparison to the marked ROI is shown.

As the result, the mean accuracy of 0.745 is obtained (to the "Dice Score" or F1-score measure, meaning harmonic mean between accuracy and comprehensiveness). The model was evaluated on testing data set of 600 images. In order to visualize the obtained results, the byte masks, obtained by manual segmentation, and the ones, predicted by the model, were compared. The difference between them is shown in Fig. 6.

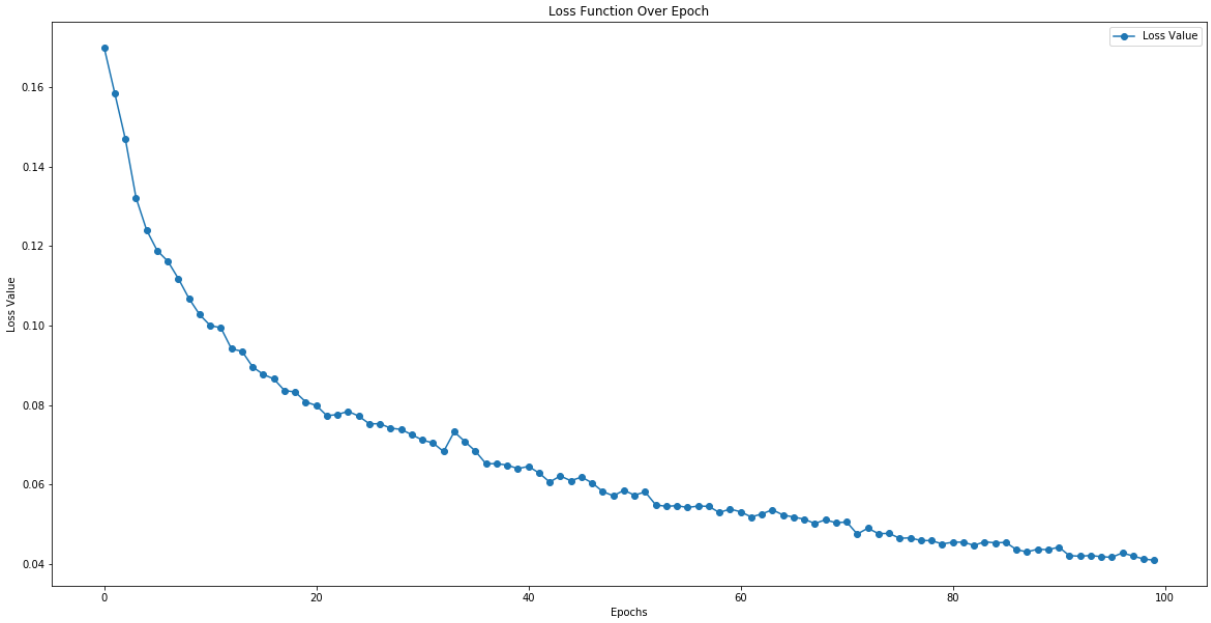

Fig. 5. **Loss Function by epochs**
***Source*: compiled by the author**

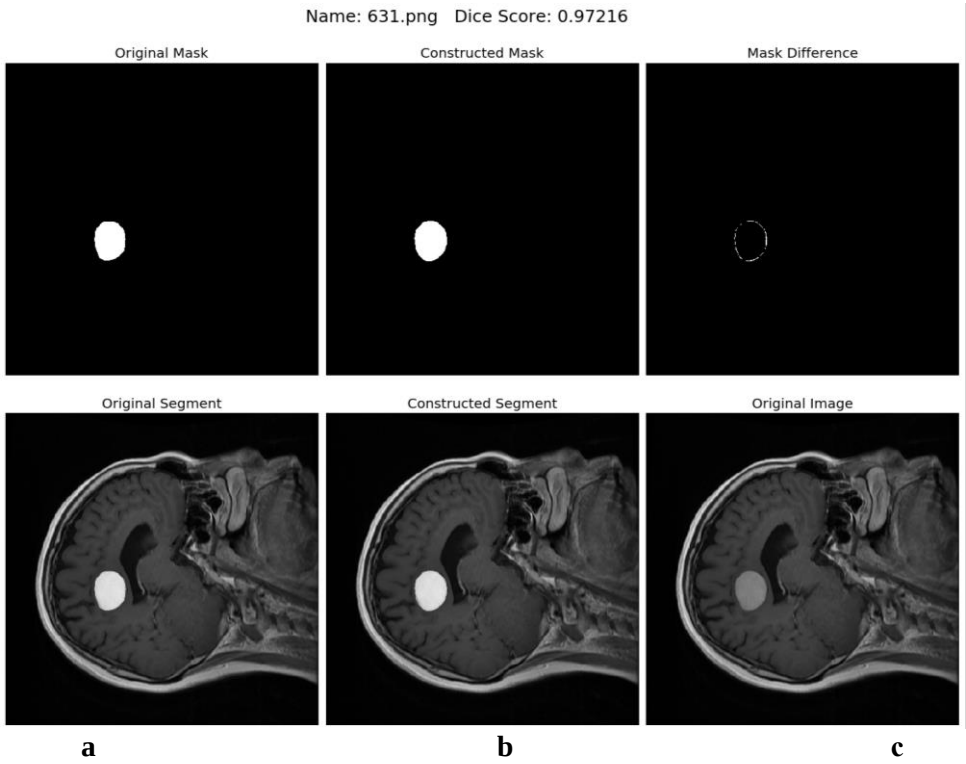

a **b** **c**

Fig. 6. **Comparison of segmentations:**
a – original byte mask; b – byte mask given by model; c – the difference between two masks
***Source*: compiled by the author**

MRI IMAGES CLASSIFICATION

To build models, which classify MRI images, the texture features were taken, proposed by other authors from the Department of Biomedical Cybernetics, National Technical University of Ukraine "Igor Sikorsky Kyiv Polytechnic Institute" [29-30]. They were invented in the context of liver ultrasound image classification task. Nevertheless, since the features were intended for image texture analysis, there should be no principal difference about the type of images these features are used for. This way, in the case of successful feature use for this task, it is possible to make a conclusion that invented features by the authors are universal and can be widely used for any medical images.

Used features can be divided into the following groups:

1. Patented features, based on grey level co-occurrence matrix (GLCM): x_1 – frequency rate stability range in the region of low-intensity greyscale combinations; x_2 – neighbor pixels greyscale combination incidence, which distinguishes the liver images in norma and pathology in the best way; x_3 – maximum greyscale value to the level of significance.

2. The features, obtained with the help of spatial sweep (works on the principle of group method of data handling).

3. Statistical features obtained from images on a single scale. To bring the images to a single scale, the authors [30] invented horizontal and vertical differentiation matrices. However, these matrices were used for ROI, which are presented as rectangular matrices. Since the ROI that are distinguished by the automatic segmentation model are presented in the form of a certain curvilinear Figure (Fig. 7), these matrices are not exactly suitable and need to be modified.

Since grayscale pixels in this area are recorded in a one-dimensional array to obtain information on ROI, the differentiation version shown in Fig. 8 can be used. 4. Ensembles of grayscale pairs, which best differentiate brain tumors in images on a single scale by differentiation (Fig. 8). Differential GLCMs were constructed separately for each task "One against All".

The task "One versus All" implies that classification models will be built for different types of tumors ("Meningioma versus All", "Glioma versus All" and "Pituitary tumor versus All"), i.e. the task of multiclass classification is reduced to three binary classification tasks.

As a result of the construction of difference GLCMs and the use of a genetic algorithm, the following optimal (after criterion (1) of correlation feature selection; since grayscale pairs have a quantitative frequency characteristic, the Spearman correlation was used) ensembles of grayscale pairs were obtained (Table 1).

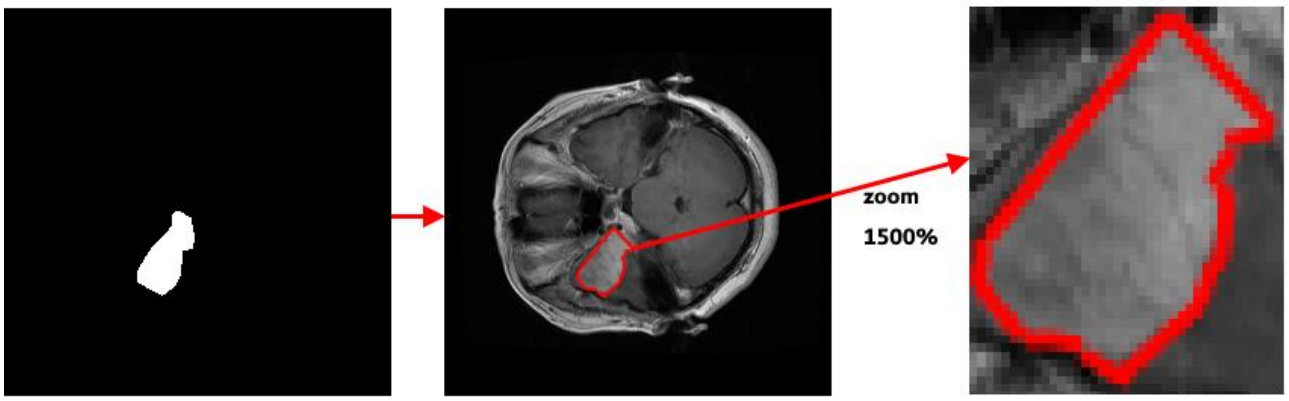

Fig. 7. **Selection of the area of greyscale pixels by byte mask**
***Source*: compiled by the author**

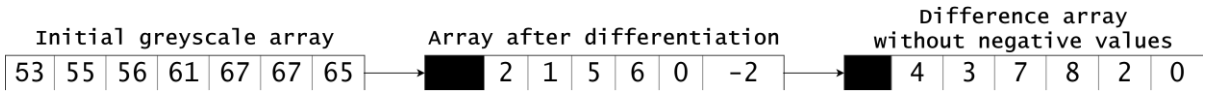

Fig. 8. **Array differentiation**
***Source*: compiled by the author**

ISSN 2663-0176 (Print)
ISSN 2663-7731 (Online)

Table 1. **Optimal ensembles of greyscale pairs**

Classification task	Ensemble of greyscale pairs	Average recognition accuracy
Meningioma versus all	[(27, 25); (32, 34); (37, 38); (46, 48); (69, 69); (69, 70); (70, 68)]	71.3 %
Glioma versus all	[(42, 43); (74, 71); (76, 73); (80, 76); (80, 77); (86, 83); (91, 92); (96, 93)]	61.7 %
Pituitary tumor versus all	[(76, 81); (77, 82); (81, 85); (87, 82); (87, 91); (104, 102); (106, 103); (106, 107); (106, 109); (108, 104); (109, 108)]	69.4 %

***Source*: compiled by the author**

The values for the last column were obtained as follows: for each grayscale pair, thresholds were found in the ensemble, which are best divided into norms and pathology, and then the recognition accuracy was calculated

$$S_k = \frac{k\overline{r_{cf}}}{\sqrt{k + k(k-1)\overline{r_{ff}}}}, \quad (1)$$

where: $\overline{r_{cf}}$ – the average value of correlation modules of all grayscale pairs with a dependent variable (class of object); $\overline{r_{ff}}$ – the average value of correlation modules of all grayscale pairs among themselves; k – number of grayscale pairs in the ensemble.

Having created a common feature stack, they were used to obtain three classification models in "One versus All" task. The classification was done with the help of Random Forest algorithm. Before classification, the total sample was divided into: training (70 %), testing (20 %), and examining (10 %) ones. Each model was evaluated by accuracy values, positive (share of correctly predicted first class objects) and negative (share of correctly predicted second class objects) predictive values. The results are shown in Table 2.

As well as the random forest can solve the multiple class classification task, the model was created, which defines each of the three tumor types separately as a class. The results are shown in Table 3.

By comparing the positive and negative predictive values on the examining sample obtained by the "One versus All" models and the model for the multiclass problem, it can be concluded that the Random Forest is more advantageous to use for obtaining individual "One versus All" models than for the multiclass problem.

In order to understand the effectiveness of the features suggested by colleagues, a comparison was made between them and such well-known texture features as Haralick's [31]. These features are calculated from GLCM. Haralick proposed only 14 features, each of which is described in Fig. 9.

New Random Forest models were built based on these features. Their evaluation is shown in Table 4.

By comparing the results, we can see that the Random Forest, built on the features of our colleagues, gives better results in the examining sample. However, if we compare the results obtained in the testing sample, the results are not so unequivocal. This pushed us to combine all the features (both suggested by our colleagues and Halarick's) into one common stack. In this way, the Goethe quote was implemented: "*Divide and conquer" is a strong statement, but "Unite and lead" is wiser* ©. By building Random Forest on this stack, the best results were achieved, as described in Table 5.

A comparative bar chart (Fig. 10) was constructed to show the differences in the models obtained from various groups of features. Evaluation values were taken from examining sample.

Fig. 10 clearly shows that by combining all the texture features, the best MRI classification results can be achieved.

Table 2. **Evaluation of resulted Random Forests**

Task	Training sample (70%)			Testing sample (20 %)			Examining sample (10 %)		
	Accuracy	PPV	NPV	Accuracy	PPV	NPV	Accuracy	PPV	NPV
Meningioma versus all	100 %	1	1	88.6 %	0.942	0.7	92.2 %	0.983	0.718
Glioma versus all	100 %	1	1	93.8 %	0.938	0.922	93.8 %	0.993	0.874
Pituitary tumor versus all	100 %	1	1	86.3 %	0.92	0.84	84 %	0.902	0.699

***Source*: compiled by the author**

Table 3. **Evaluation of multiclass Random Forest**

Sample	Accuracy	PPV			NPV		
		1st class (meningioma)	2nd class (glioma)	3rd class (pituitary tumor)	1st class (meningioma)	2nd class (glioma)	3rd class (pituitary tumor)
Training (70 %)	100 %	1	1	1	1	1	1
Testing (20 %)	85 %	0.946	0.944	0.887	0.743	0.922	0.821
Examining (10 %)	85.7 %	0.936	0.945	0.907	0.803	0.923	0.796

***Source*: compiled by the author**

Angular Second Moment	$\sum_i \sum_j p(i,j)^2$
Contrast	$\sum_{n=0}^{N_g-1} n^2 \{\sum_{i=1}^{N_g} \sum_{j=1}^{N_g} p(i,j)\}, \lvert i-j \rvert = n$
Correlation	$\frac{\sum_i \sum_j (ij) p(i,j) - \mu_x \mu_y}{\sigma_x \sigma_y}$ where μ_x , μ_y , σ_x , and σ_y are the means and std. deviations of p_x and p_y , the partial probability density functions
Sum of Squares: Variance	$\sum_i \sum_j (i-\mu)^2 p(i,j)$
Inverse Difference Moment	$\sum_i \sum_j \frac{1}{1+(i-j)^2} p(i,j)$
Sum Average	$\sum_{i=2}^{2N_g} i p_{x+y}(i)$ where x and y are the coordinates (row and column) of an entry in the co-occurrence matrix, and $p_{x+y}(i)$ is the probability of co-occurrence matrix coordinates summing to $x+y$
Sum Variance	$\sum_{i=2}^{2N_g} (i - f_8)^2 p_{x+y}(i)$
Sum Entropy	$-\sum_{i=2}^{2N_g} p_{x+y}(i) \log\{p_{x+y}(i)\} = f_8$
Entropy	$-\sum_i \sum_j p(i,j) log(p(i,j))$
Difference Variance	$\sum_{i=0}^{N_g-1} i^2 p_{x-y}(i)$
Difference Entropy	$-\sum_{i=0}^{N_g-1} p_{x-y}(i) \log\{p_{x-y}(i)\}$
Info. Measure of Correlation 1	$\frac{HXY - HXY1}{\max\{HX, HY\}}$
Info. Measure of Correlation 2	$(1 - \exp[-2(HXY2 - HXY)])^{\frac{1}{2}}$ where $HXY = -\sum_i \sum_j p(i,j) \log(p(i,j))$, HX , HY are the entropies of p_x and p_y , $HXY1 = -\sum_i \sum_j p(i,j) \log\{p_x(i) p_y(j)\}$ $HXY2 = -\sum_i \sum_j p_x(i) p_y(j) \log\{p_x(i) p_y(j)\}$
Max. Correlation Coeff.	Square root of the second largest eigenvalue of $\mathbf{Q}$ where $\mathbf{Q}(i,j) = \sum_k \frac{p(i,k) p(j,k)}{p_x(i) p_y(k)}$

Fig. 9. **Haralick texture features**
***Source*: http://murphylab.web.cmu.edu/publications/boland/boland_node26.html**

ISSN 2663-0176 (Print)
ISSN 2663-7731 (Online)

Table 4. **Evaluation of resulted Random Forests based on Haralick texture features**

Task	Training sample (70 %)			Testing sample (20 %)			Examining sample (10 %)		
	Accuracy	PPV	NPV	Accuracy	PPV	NPV	Accuracy	PPV	NPV
Meningioma versus all	100 %	1	1	90.1 %	0.957	0.714	89.9 %	0.953	0.718
Glioma versus all	100 %	1	1	94.4 %	0.978	0.904	91.5 %	0.963	0.86
Pituitary tumor versus all	100 %	1	1	86.2 %	0.939	0.865	82.4 %	0.907	0.634

***Source*: compiled by the author**

Table 5. **Evaluation of resulted Random Forests based on all texture features**

Task	Training sample (70 %)			Testing sample (20 %)			Examining sample (10 %)		
	Accuracy	PPV	NPV	Accuracy	PPV	NPV	Accuracy	PPV	NPV
Meningioma versus all	100 %	1	1	90.6 %	0.97	0.693	92.5 %	0.97	0.775
Glioma versus all	100 %	1	1	93.4 %	0.969	0.894	94.8 %	0.994	0.895
Pituitary tumor versus all	100 %	1	1	85.2 %	0.91	0.717	86 %	0.916	0.731

***Source*: compiled by the author**

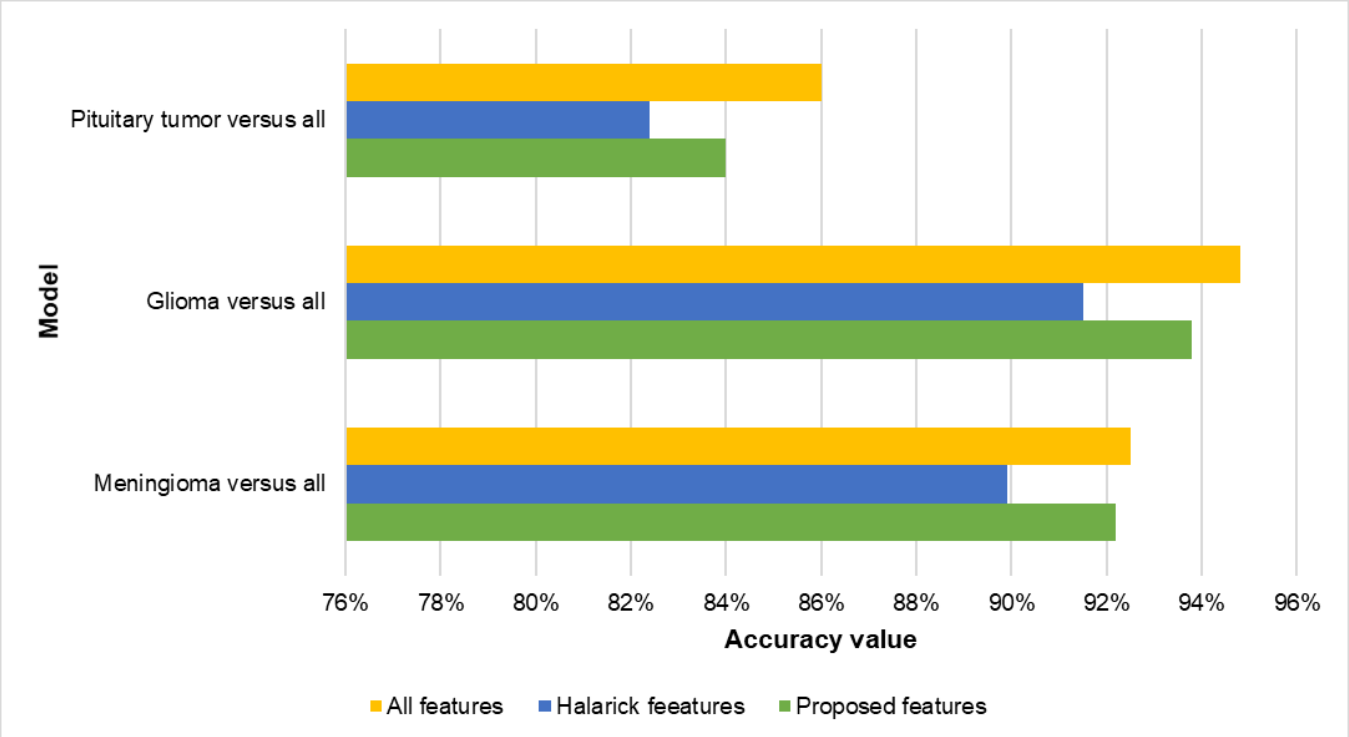

Fig. 10. **Comparative bar chart**
***Source*: compiled by the author**

CONCLUSION

As a result of this work, a model of automatic brain MRI segmentation using the architecture of the U-Net deep convolution neural network was trained. The obtained model on a testing sample of 600 images to 74.5 % reproduce the manual segmentation of images.

After obtaining the model, the texture features proposed by colleagues from the Department of Biomedical Cybernetics were calculated on the segmented images. They were used to obtain three models of "One versus All" classification and one model of a multiclass task using a Random Forest classification algorithm. A comparison of the results showed that the Random Forest is better used for individual "One versus All" tasks than for the multiclass task.

New models of the "One versus All" classification were then built on the Haralick texture features, which are well known for this kind of task. This was done to compare them with features proposed by colleagues. As a result, it turned out that better results were given by the proposed features but combining them with the Haralick features in one common stack gave the best results on the examining sample (10 %). Thus, it can be said that the texture features, which were developed by colleagues in the context of the liver ultrasound images classifying task can occur in almost any task of classifying medical images and are kind of universal. However, a lot of research needs to be done to give a final verdict.

REFERENCES

1. de Zwart, A. D., Beeres, F. J. P., Rhemrev, S. J., Bartlema, K. & Schipper, I. B. "Comparison of MRI, CT and Bone Scintigraphy for Suspected Scaphoid Fractures". *Journal "European Journal of Trauma and Emergency Surgery".* 2016; 42(6): 725–731. DOI: https://doi.org/10.1007/s00068-015-0594-9.

2. Verma, A. & Khanna, G. "A Survey on Digital Image Processing Techniques for Tumor Detection". *Journal "Indian J Sci Technol".* 2016; 9(14): 15 p. DOI: https://doi.org/10.17485/ijst/2016/v9i14/84976.

3. Zandifar, A., Fonov, V., Coupé, P., Pruessner, J. & Collins, D. L. "A Comparison of Accurate Automatic Hippocampal Segmentation Methods". *Neuroimage*. 2017; 155: 383–393. DOI: https://doi.org/10.1016/j.neuroimage.2017.04.018.

4. Jelercic, S. & Rajer, M. "The Role of PET-CT in Radiotherapy Planning of Solid Tumours". *"Radiology and Oncology"*. 2015; Vol. 49: 1–9. DOI: https://doi.org/10.2478/raon-2013-0071.

5. Torigian, D. A., Zaidi, H., Kwee, T. C., Saboury, B., Udupa, J. K., Cho, Z. H., et al. "PET/MR Imaging: Technical Aspects and Potential Clinical Applications". *Journal Radiology*. 2013; 267(1): 26–44. DOI: https://doi.org/10.1148/radiol.13121038.

6. Zhao, B., Schwartz, L. H. & Larson, S. M. "Imaging Surrogates of Tumor Response to Therapy: Anatomic and Functional Biomarkers". *Journal J Nucl Med.* 2009; 50(2): 239–249. DOI: https://doi.org/10.2967/jnumed.108.056655.

7. Liu, X., Deng, Z. & Yang, Y. "Recent Progress in Semantic Image Segmentation". *Journal Artif Intell Rev*. 2019; 52(2): 1089–1106. DOI: https://doi.org/10.1007/s10462-018-9641-3.

8. Chun-Xiang, W., Yao, W. & Zhi-Bo, H. "Segmentation Adaptive Slicing Algorithm Based on Features of Parts in Additive Manufacturing". *Journal Chinese J Eng Des*. 2020; 27(3): 373–379. DOI: https://doi.org/10.3785/j.issn.1006-754X.2020.00.038.

9. Acuff, S. N., Jackson, A. S., Subramaniam, R. M. & Osborne, D. "Practical Considerations for Integrating PET/CT into Radiation Therapy Planning". *Journal J Nucl Med Technol*. 2018; 46(4): 343–348. DOI: https://doi.org/10.2967/jnmt.118.209452.

10. Werner-Wasik, M., Nelson, A. D., Choi, W., Arai, Y., Faulhaber, P. F., Kang, P., et al. "What is the Best Way to Contour Lung Tumors on PET Scans? Multiobserver validation of a gradient-based method using a NSCLC digital PET phantom". *Int J Radiat Oncol Biol Phys*. 2012; 82(3): 1164–1171. DOI: https://doi.org/10.1016/j.ijrobp.2010.12.055.

11. Bagci, U., Udupa, J. K., Mendhiratta, N., Foster, B., Xu, Z., Yao, J., et al. "Joint Segmentation of Anatomical and Functional Images: Applications in Quantification of Lesions from PET, PET-CT, MRI-PET, and MRI-PET-CT Images". *Journal Med Image Anal*. 2013; 17(8): 929–945. DOI: https://doi.org/10.1016/j.media.2013.05.004.

12. Khalil, M. M. "Basic Science of PET Imaging". *Journal Basic Science of PET Imaging*. 2016. 619 p.

13. Ambrosini, V., Fanti, S., Chengazi, V. U. & Rubello, D. "Diagnostic Accuracy of FDG PET/CT in Mediastinal Lymph Nodes from Lung Cancer". *European Journal of Radiology*. 2014; Vol.83: 1301–1302. DOI: https://doi.org/10.1016/j.ejrad.2014.04.035.

14. Toledano, M. N., Vera, P., Tilly, H., Jardin, F. & Becker, S. "Comparison of Therapeutic Evaluation Criteria in FDG-PET/CT in Patients with Diffuse Large-cell B-cell Lymphoma: Prognostic Impact of Tumor/liver ratio". *PLoS One.* 2019; 14(2): 16 p. DOI: https://doi.org/10.1371/journal.pone.0211649.

ISSN 2663-0176 (Print)
ISSN 2663-7731 (Online)

15. Delbeke, D., Coleman, R. E., Guiberteau, M. J., Brown, M. L., Royal, H. D., Siegel, B. A, et al. “Procedure Guideline for Tumor Imaging with 18F-FDG PET/CT 1.0”. *Journal of Nuclear Medicine*. 2006; Vol.47: 885–895.

16. Jones, J. L., Xie, X. & Essa, E. “A Shortest Path Approach to Interactive Medical Image Segmentation”. *In: Biomedical Image Segmentation: Advances and Trends.* 2016. p. 407–436. DOI: https://doi.org/10.1201/9781315372273.

17. Chen, X. & Pan, L. “A Survey of Graph Cuts/Graph Search Based Medical Image Segmentation”. *IEEE Rev Biomed Eng*. 2018; 11: 112–124. DOI: https://doi.org/10.1109/RBME.2018.2798701.

18. Li, G., Jiang, D., Zhou, Y., Jiang, G., Kong, J. & Manogaran, G. “Human Lesion Detection Method Based on Image Information and Brain Signal”. *IEEE Access.* 2019; 7: 11533–11542. DOI: https://doi.org/10.1109/ACCESS.2019.2891749.

19. Yu, K., Shi, F., Gao, E., Zhu, W., Chen, H. & Chen, X. “Shared-hole Graph Search with Adaptive Constraints for 3D Optic Nerve Head Optical Coherence Tomography Image Segmentation”. *Journal Biomed Opt Express.* 2018; 9(3): 962 p. DOI: https://doi.org/10.1364/boe.9.000962.

20. Meskini, E., Helfroush, M. S., Kazemi, K. & Sepaskhah, M. “A New Algorithm for Skin Lesion Border Detection in Dermoscopy Images”. *Journal J Biomed Phys Eng*. 2018; 8(1): 109–118. DOI: 10.22086/jbpe.v0i0.444.

21. Dey, N., Rajinikanth, V., Ashour, A. S. & Tavares, J. M. R. S. “Social group Optimization Supported Segmentation and Evaluation of Skin Melanoma Images”. *Symmetry (Basel).* 2018; 10(2): 21 p. DOI: https://doi.org/10.3390/sym10020051.

22. Feng, X., Qing, K., Tustison, N. J., Meyer, C. H. & Chen, Q. “Deep Convolutional Neural Network for Segmentation of Thoracic Organs-at-risk Using Cropped 3D Images”. *Journal Med Phys.* 2019; 46 (5): 2169–2180. DOI: https://doi.org/10.1002/mp.13466.

23. Iglovikov, V. & Shvets, A. “TernausNet: U-Net with VGG11 Encoder Pre-Trained on ImageNet for Image Segmentation”. *Journal ArXiv.* 2018. 5 p.

24. Ronneberger, O., Fischer, P. & Brox, T. “U-net: Convolutional Networks for Biomedical Image Segmentation”. *In: Lecture Notes in Computer Science (including subseries Lecture Notes in Artificial Intelligence and Lecture Notes in Bioinformatics).* 2015. p. 234–241. DOI: https://doi.org/10.1007/978-3-319-24574-4_28.

25. Zhou, J., Zhang, Q., Zhang, B. & Chen, X. “TongueNet: A Precise and Fast Tongue Segmentation System Using U-net with a Morphological Processing Layer”. *Journal Appl Sci.* 2019; 9(15): 19 p. DOI: https://doi.org/10.3390/app9153128.

26. Lai, X., Yang, W. & Li, R. “DBT Masses Automatic Segmentation Using U-Net Neural Networks”. *Comput Math Methods Med*. 2020; 2020: 10p. DOI: 10.1155/2020/7156165.

27. Cheng, J., Huang, W., Cao, S., Yang, R., Yang, W., Yun, Z., et al. “Enhanced Performance of Brain Tumor Classification via Tumor Region Augmentation and Partition”. *Journal PLoS One.* 2015; 10(10): 13 p. DOI: https://doi.org/10.1371/journal.pone.0140381.

28. Cheng, J., Yang, W., Huang, M., Huang, W., Jiang, J., Zhou, Y., et al. “Retrieval of Brain Tumors by Adaptive Spatial Pooling and Fisher Vector Representation”. *Journal PLoS One*. 2016; 11(6): 15 p. DOI: https://doi.org/10.1371/journal.pone.0157112.

29. Kruglyi, V. & Nastenko, Ie. “Formirovanie informativnih priznakov dlia zadachi klassifikaciyi patologiya/norma po izobrajeniyu UZI pecheni pacienta” (in Russian). *Journal Scientific Discussion*. 2019; 1(31): 57–59.

30. Nastenko, Ie., Dykan, I., Tarasiuk, B., Pavlov, V., Nosovets, O., Babenko, V., Kruglyi, V., Dyba, M. & Soloduschenko, V. “Klassifikaciya staniv pechinki pri difuznih zahvoruvanniah na osnovi statistichnih pokaznikiv teksturi ultrazvukovih zobrazhen’ ta MGUA” (in Ukrainian). *Journal Induktivne modelliuvannia skladnih sistem*. 2019; 11: 54–66.

31. Brynolfsson, P., Nilsson, D., Torheim, T., Asklund, T., Karlsson, C. T., Trygg, J., et al. “Haralick Texture Features from Apparent Diffusion Coefficient (ADC) MRI images depend on imaging and pre-processing parameters”. *Sci Rep.* 2017; 7(1): 11 p. DOI: https://doi.org/10.1038/s41598-017-04151-4.

Conflicts of Interest: the authors declare no conflict of interest

Received 08.10.2020
Received after revision 13.11.2020
Accepted 20.11. 2020

DOI: https://doi.org/10.15276/aait.04.2020.4
UDC 004.9 + 616-079.4

КЛАСИФІКАЦІЯ МРТ ЗОБРАЖЕНЬ МОЗКУ З ВИКОРИСТАННЯМ АВТОМАТИЧНОЇ СЕГМЕНТАЦІЇ І ТЕКСТУРНОГО АНАЛІЗУ

Анастасія Вікторівна Карлюк[1)]
ORCID: https://orcid.org/0000-0001-7011-7237, karliukanastasia@gmail.com
Євген Арнольдович Настенко[1)]
ORCID: https://orcid.org/0000-0002-1076-9337, nastenko.e@gmail.com
Олена Костянтинівна Носовець[1)]
ORCID: https://orcid.org/0000-0003-1288-3528, o.nosovets@gmail.com
Віталій Олегович Бабенко[1)]
ORCID: https://orcid.org/0000-0002-8433-3878, vbabenko2191@gmail.com
[1)] Національный технічний університет України «Київський політехнічний інститут імені Ігоря Сікорського», вул. Михайла Брайчевського 5а, Київ, Україна

АНОТАЦІЯ

Пухлина мозку є доволі тяжкою формою захворювання людини. Його своєчасне виявлення, а також визначення конкретного типу пухлини, є актуальною задачею в сучасній медицині. Для визначення пухлини останнім часом використовують методи сегментації на трьохвимірних зображеннях мозку, таких як комп'ютерна чи магнітно-резонансна томографія. Однак, зазвичай сегментацію проводять вручну, через що тратиться немала кількість часу, до того ж все залежить від досвіду лікаря. В даній роботі розглядається можливість створення методу для автоматичної сегментації зображень. В якості навчальної вибірки була взята медична база магнітно-резонансних томографій мозку з трьома типами пухлин: менінгіома, гліома і пухлина гіпофізу. З врахування різних зрізів база мала в наявності: 708 прикладів менінгіоми, 1426 прикладів гліоми і 930 прикладів пухлини гіпофізу. Авторами бази були розмічені області інтересу на кожному знімку, що було використано в якості вчителя для моделі автоматичної сегментації. Перед тим як створювати модель були проаналізовані існуючи на даний момент популярні методи сегментації. В якості найбільш підходящого для поставленої в дослідженні задачі методу автоматичної сегментації була взята архітектура глибокої згорткової нейронної мережі U-Net. В результаті її використання була отримана модель, яка на тестовій вибірці із шістсот знімків зуміла в сімдесяти чотирьох процентах випадків правильно відсегментувати зображення. Після отримання моделі автоматичної сегментації, для класифікації пухлин мозку були побудовані моделі «випадкового лісу» для трьох задач «один проти всіх», а також для мультикласової задачі. Перед побудовою моделей загальні вибірки були поділені на навчальну (70 %), тестову (20 %) і екзаменаційну (10 %). На екзаменаційній вибірці точність моделей варіюється від 84 до 94 відсотків. Для побудови класифікаційних моделей використовувались ознаки, отримані за методами текстурного аналізу, і яку були розроблені співавторами із кафедри Біомедичної кібернетики в задачі класифікації ультразвукових досліджень печінки. Вони також були порівняні з загальновідомими текстурними ознаками Харалiка. Порівняння показало, що кращий спосіб домогтися точної моделі класифікації, це об'єднати всі ознаки в один стек.

Ключові слова: класифікація; «один проти всіх»; мультикласова задача; автоматична сегментація; текстурний аналіз; пухлина; магнітно-резонансна томографія

DOI: https://doi.org/10.15276/aait.04.2020.4
UDC 004.9 + 616-079.4

КЛАССИФИКАЦИЯ МРТ ИЗОБРАЖЕНИЙ МОЗГА С ИСПОЛЬЗОВАНИЕМ АВТОМАТИЧЕСКОЙ СЕГМЕНТАЦИИ И ТЕКСТУРНОГО АНАЛИЗА

Анастасия Викторовна Карлюк[1)]
ORCID: https://orcid.org/0000-0001-7011-7237, karliukanastasia@gmail.com
Евгений Арнольдович Настенко[1)]
ORCID: https://orcid.org/0000-0002-1076-9337, nastenko.e@gmail.com
Елена Константиновна Носовец[1)]
ORCID: https://orcid.org/0000-0003-1288-3528, o.nosovets@gmail.com
Виталий Олегович Бабенко[1)]
ORCID: https://orcid.org/0000-0002-8433-3878, vbabenko2191@gmail.com
[1)] Национальный технический университет Украины «Киевский политехнический институт имени Игоря Сикорского», ул. Михаила Брайчевского 5а, Киев, Украина

АННОТАЦИЯ

Опухоль мозга является достаточно тяжелым видом заболевания человека. Его своевременное обнаружение, а также определение конкретного типа опухоли, является актуальной задачей в современной медицине. Для определения опухоли в последнее время используют методы сегментации на трёхмерных изображениях мозга, таких как компьютерная или

ISSN 2617-4316 (Print)
ISSN 2663-7723 (Online)

магнитно-резонансная томография. Однако, обычно сегментацию проводят вручную, из-за чего тратится немалое количество времени, к тому же всё зависит от опыта врача. В данной работе рассматривается возможность создания метода для автоматической сегментации изображений. В качестве обучающей выборки была взята медицинская база магнитно-резонансных томографий мозга с тремя типами опухолей: менингиома, глиома и опухоль гипофиза. С учетом различных срезов база имела в наличии: 708 примеров менингиомы, 1426 примеров глиомы и 930 примеров опухоли гипофиза. Авторами базы были размечены области интереса на каждом снимке, что было использовано в качестве учителя для модели автоматической сегментации. Прежде чем создать модель, были проанализированы существующие на данный метод популярные методы сегментации. В качестве наиболее подходящего для поставленной в исследовании задачи метода автоматической сегментации была взята архитектура глубокой свёрточной нейронной сети U-Net. В результате её использования была получена модель, которая на тестовой выборке из шестисот снимков сумела в семидесяти четырех процентах случаев правильно отсегментировать изображение. После получения модели автоматической сегментации, для классификации опухолей мозга были построены модели «случайного леса» для трёх задач «один против всех», а также для мультиклассовой задачи. Перед построением моделей общие выборки были поделены на обучающую (70 %), тестовую (20 %) и экзаменационную (10 %). На экзаменационной выборке точность моделей варьируется от 84 до 94 процентов. Для построения классификационных моделей использовались признаки, полученные за методами текстурного анализа, и которые были разработаны соавторами из кафедры Биомедицинской кибернетики в задаче классификации ультразвуковых исследований печени. Они также были сравнены с общеизвестными текстурнымипризнаками Харалика. Сравнение показало, что лучший способ добиться точной модели классификации, это объединить все признаки в один стек.

Ключевые слова: классификация; «один против всех»; мультиклассовая задача; автоматическая сегментация; текстурный анализ; опухоль; магнитно-резонансная томография

ABOUT THE AUTHORS

Anastasia Viktorivna Karliuk – Department of Biomedical Cybernetics, National Technical University of Ukraine "Igor Sikorsky Kyiv Polytechnic Institute", 5a, Mikhail Braichevsky St. Kyiv, Ukraine
karliukanastasia@gmail.com. ORCID: https://orcid.org/0000-0001-7011-7237.
Research field: Information Technologies in Medicine; Computer Science; Data Science Deep Learning; Computer Vision

Анастасія Вікторівна Карлюк – кафедра Біомедичної кібернетики Національного технічного університету України «Київський політехнічний інститут імені Ігоря Сікорського», вул. Михайла Брайчевського 5а. Київ, Україна

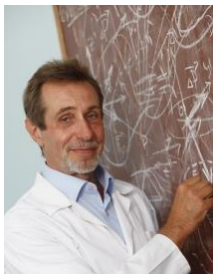

Ievgen Arnoldovich Nastenko – Doctor of Biological Sciences (2008), Candidate of Technical Sciences (1989), Senior Research Officer. Head of Department of the Department of Biomedical Cybernetics, National Technical University of Ukraine "Igor Sikorsky Kyiv Polytechnic Institute", 5a Mikhail Braichevsky St. Kyiv, Ukraine
nastenko.e@gmail.com. ORCID: https://orcid.org/0000-0002-1076-9337
***Research field*:** Life Science; Data Mining; Nonlinear Dynamic Methods; Mathematical Modeling; Biomedical Data Digital Processing; Data Science

Євген Арнольдович Настенко – доктор біологічних наук (2008), кандидат технічних наук (1989), старший науковий співробітник, зав. кафедрой Біомедичної кібернетики Національного технічного університету України «Київський політехнічний інститут імені Ігоря Сікорського», вул. Михайла Брайчевського 5а. Київ, Україна

Olena Kostiantinivna Nosovets – Candidate of Technical Sciences (2015), Associate Professor of the Department of Biomedical Cybernetics, National Technical University of Ukraine "Igor Sikorsky Kyiv Polytechnic Institute", 5a, Mikhail Braichevsky St. Kyiv, Ukraine
o.nosovets@gmail.com.ORCID: https://orcid.org/0000-0003-1288-3528
***Research field*:** Information Technologies in Medicine; Computer Science; Data Science; Deep Learning

Олена Костянтинівна Носовець – кандидат технічних наук (2015), доцент кафедры Біомедичної кібернетики Національного технічного університету України «Київський політехнічний інститут імені Ігоря Сікорського», вул. Михайла Брайчевського 5а. Київ, Україна

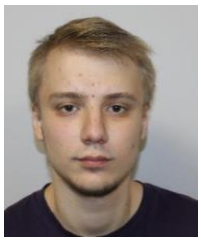

Vitalii Olegovich Babenko – Department of Biomedical Cybernetics, National Technical University of Ukraine "Igor Sikorsky Kyiv Polytechnic Institute", 5a Mikhail Braichevsky St. Kyiv, Ukraine
vbabenko2191@gmail.com. ORCID: https://orcid.org/0000-0002-8433-3878.
Research field: Information Technologies in Medicine; Computer Science; Data Science; Deep Learning

Віталій Олегович Бабенко – кафедра Біомедичної кібернетики Національного технічного університету України «Київський політехнічний інститут імені Ігоря Сікорського», вул. Михайла Брайчевського 5а. Київ, Україна